The complete solution of Alt-Burmester synthesis problems for four-bar linkages

Daniel A. Brake*[1], Jonathan D. Hauenstein†[1], Andrew P. Murray‡[2], David H. Myszka§[2] and Charles W. Wampler¶[3]

[1]Department of Applied and Computational Mathematics and Statistics, University of Notre Dame
[2]Department of Mechanical Engineering, University of Dayton
[3]General Motors R&D Center

December 7, 2015

Abstract

Precision-point synthesis problems for design of four-bar linkages have typically been formulated using two approaches. The exclusive use of path-points is known as "path synthesis", whereas the use of poses, i.e. path-points with orientation, is called "rigid-body guidance" or the "Burmester problem". We consider the family of "Alt-Burmester" synthesis problems, in which some combination of path-points and poses are specified, with the extreme cases corresponding to the typical approaches.

The Alt-Burmester problems that have, in general, a finite number of solutions include Burmester's original five-pose problem and also Alt's problem for nine path-points. The elimination of one path-point increases the dimension of the solution set by one, while the elimination of a pose increases it by two. Using techniques from numerical algebraic geometry, we tabulate the dimension and degree of all problems in this Alt-Burmester family, and provide more details concerning all the zero- and one-dimensional cases.

1 Introduction

In linkage design, dimensional synthesis consists of determining the dimensions of a prespecified type of linkage such that the designed mechanism performs a desired

*danielthebrake@gmail.com
†hauenstein@nd.edu
‡murray@udayton.edu
§dmyszka@udayton.edu
¶charles.w.wampler@gm.com

task [1, 2]. Traditionally, the task specification falls into one of three categories: function generation, path-point generation, and motion generation. Function generation, which we do not treat in this paper, seeks to coordinate the rotations of two or more joint angles. Path-point generation seeks to move a reference point on one of the links along a prescribed path, i.e., for planar linkages, the task is to move along a curve in $\mathbb{R}^2$. Motion generation, also known as rigid-body guidance, seeks to move one of the links along a prescribed trajectory of position and orientation, i.e., for planar linkages, the task is a motion along a curve in $SE(2)$. We will use "pose" to mean a point in $SE(2)$.

Since a linkage has only a finite number of kinematic parameters that can be adjusted, such as link lengths, exactly matching an arbitrary continuous task curve is not possible. One alternative is to consider a dimensional synthesis problem that prescribes a finite number of *precision points* along the task curve. Solutions of the problem are linkages that interpolate the precision points. For each type of linkage and task, there is a maximum number of precision points that can be arbitrarily prescribed. If fewer than this number are prescribed, the dimension of the solution set increases allowing freedom of choice that the designer may use to satisfy other criteria. Solutions of the precision-point problem must be further examined for their suitability, such as checking for acceptable motion between the precision points, detecting branch and circuit defects, evaluating transmission characteristics, and assessing sensitivity to dimensional variation. (For discussion on such issues, see [1, 3, 4]). Our current focus is the precision-point synthesis phase of the design process.

We specifically consider dimensional synthesis problems for planar four-bar linkages. Instead of pure path-point generation or pure motion generation, we treat tasks specified with a mix of precision path-points and precision poses, as was first considered in [5]. Whereas Alt [6] was an early proponent of four-bar path generation while classical motion generation for planar four-bars is often called a Burmester [7] problem, we call this generalized type of synthesis an "Alt-Burmester" problem. Varying the number of path-points and poses gives 25 problem types in all, five of which have isolated solutions and four of which have solution curves. We give the dimension and degree of the solution set for all cases up to and including the maximal number of precision points, and give extra details on each case having a zero- or one-dimensional solution set.[1]

The remainder of this paper is organized as follows. Section 2 reviews the literature on precision-point synthesis of four-bars and also on numerical algebraic geometry, the numerical technique we use to solve the Alt-Burmester problems. Section 3 formulates polynomial systems for the problems, while the results of solving general cases are summarized in Section 4. Section 5 presents several particular examples in more detail with Section 6 providing a summary of our contribution.

[1] A "zero-dimensional" set is a set with a finite number of members. In other words, its solutions are isolated points.

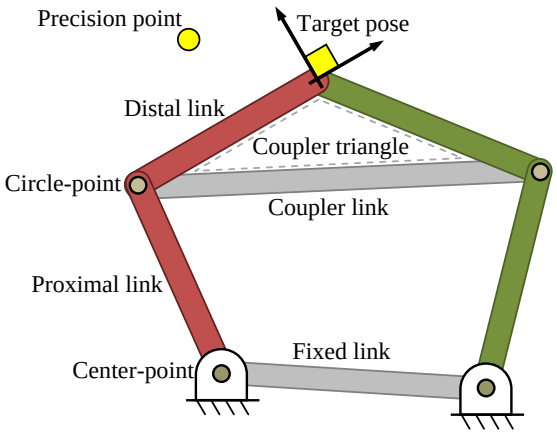

Figure 1: A planar four-bar mechanism, achieving a desired pose consisting of target point and orientation. The distal links of two RR dyads are rigidly joined, forming the coupler triangle.

2 Background

2.1 Precision-Point Synthesis of Four-Bars

As noted by Burmester [7] in 1886, when only precision poses are specified, the dimensional synthesis problem for four-bars reduces to the synthesis of a two-link, planar, revolute-revolute kinematic chain, termed an *RR dyad*. If we rigidly connect the distal links of two such dyads, the result is a four-bar linkage. Burmester showed that there are at most four RR dyads whose distal link reaches five general precision poses, so by combining any two of these dyads, one obtains at most six four-bars that solve the five-pose Burmester problem.

Burmester also solved the under-specified four-pose problem. In this case, there is a one-dimensional set of RR dyads that reach the four poses. One can independently pick any two distinct solutions in this set to form a four-bar that satisfies the specification, yielding a two-dimensional solution set. The problem can be formulated as finding the two joint centers at the first pose such that the RR dyad can reach the remaining poses. A pair of RR dyads are depicted in Fig. 1. The location of the base joint center in the fixed reference frame is called the *center point*, and the location of the distal joint center in the moving reference frame is called the *circle point*. The solution to the four-pose problem gives a *center-point curve* and a *circle-point curve*. Burmester showed that both these curves are cubics [3, 7, 8].

Path-point generation for a four-bar linkage is more challenging than rigid-body guidance because the two dyads cannot be found independently. Instead, the complete linkage must be considered all at once. Since the orientation of the coupler

link at precision points is not prescribed, there is greater freedom in the synthesis problem. There are two center points and two circle points to be determined at the initial precision point, for a total of eight unknown coordinates. Hence, including the initial point in the count the maximum number of precision path-points that can be generally prescribed is nine, a fact first observed by Alt [6].

When fewer than nine points are given, one may impose additional constraints on other aspects of the design. Depending on what kind of extra constraints are imposed, one may pose a wide variety of synthesis problems such that a finite number of solutions are expected. Often, the constraints are chosen to most conveniently simplify the problem, and alternatively they might be chosen to meet design constraints, such as limits on where the base joint can be located. Among the various possible combinations of design constraints, Freudenstein and Sandor [9] developed a closed form solution for certain 2, 3 and 4 path-point problems. Suh and Radcliffe [10] developed a method that leads to a set of simultaneous nonlinear equations, which can be numerically solved for up to 5 path-points. Morgan and the last author [11] used continuation methods to develop solutions for the problem of 5 path-points with the center points prescribed. The full 9 path-point problem was attacked with heuristic continuation approaches in [12] and [13] to produce partial solution lists, while the first complete solution was reported in [14] using a rigorous continuation formulation. That work showed that for 9 generic path-points there are a total of 4326 distinct four-bar solutions, which appear as 1442 triplets of Roberts cognates.

In this article, we consider "Alt-Burmester" synthesis problems in which a mixture of M precision poses and N precision points are given. We shall refer to any one of these as an "M pose N point problem" or simply the "(M, N) problem". Problems of this type were first posed in [5] along with some preliminary numerical results obtained using polynomial continuation. The work reported here gives a more complete treatment of this family of problems.

2.2 Numerical Algebraic Geometry

One approach that has a long record of solving problems in kinematics is polynomial continuation. Some highlights in this history are Tsai and Morgan's early demonstration that the inverse kinematics problem for general six-revolute robots has 16 solutions [15], Raghavan's demonstration that the forward kinematics of general Stewart-Gough platforms has 40 solutions [16], and, most relevant to the current discussion, the first complete solution of the nine-precision-point problem for four-bar synthesis [14].

All of the examples just cited are problems where a finite number of solutions are expected. Subsequently, polynomial continuation has been extended to include methods for dealing with polynomial systems that may have higher dimensional solution sets, such as curves, surfaces, and so on. The term *numerical algebraic geometry* has been adopted to more accurately describe the current capabilities. Papers discussing these methods as a general approach to kinematics include [17, 18]

with in-depth mathematical exposition in [19]. The book [20] describes in detail how to use the software package called `Bertini` that we used for the calculations in this paper. Curve decompositions are computed using the numerical cellular decomposition algorithm [21] in the `Bertini_real` software package [22].

The foundational idea in numerical algebraic geometry is that an algebraic curve in N-dimensional complex Euclidean space, $\mathbb{C}^N$, intersects a general hyperplane in a finite set of points, which are equal in number to the degree of the curve. More generally, in $\mathbb{C}^N$, an irreducible algebraic set, say X, of dimension m and degree d and a general linear space, say L, of dimension $N-m$ intersect in d distinct points,[2] say $W = X \cap L$. A *witness set* for X is the triplet $\{\mathbf{f}(\mathbf{x}), L, W\}$, where $\mathbf{f}(\mathbf{x})$ is a polynomial system for which X is an irreducible solution component. After computing the *witness point set* W using polynomial continuation, one has determined the degree of X by the number of points in W. This is just the beginning since, with a witness set in hand, one can perform a variety of further operations on X, such as intersecting it with other algebraic sets using diagonal intersection or regeneration [20]. Furthermore, when $\mathbf{f}(\mathbf{x};\mathbf{p})$ is a family of polynomial systems with parameters $\mathbf{p}$, one may study the general properties of the family by solving $\mathbf{f}(\mathbf{x};\mathbf{p}^*) = 0$ for random, complex parameters $\mathbf{p}^*$. For the work reported here, $\mathbf{p}$ is the set of precision path-points and poses. Once the solution is in hand for generic parameters, the solution for a particular problem for given real precision data can be found by parameter continuation [23].

A "natural projection" of a set, which we will simply call a projection from hereon, is obtained by just ignoring some coordinates. For example, if $(x(t), y(t), z(t))$ is a curve in 3-space, parameterized by t, then the projection of the curve onto the (x, y)-plane is just $(x(t), y(t))$. Of particular interest in four-bar synthesis problems is the projection of the solution set onto the coordinates of the joints. The center-point curve and circle-point curve of a four-pose Burmester problem are examples of this. Once one has a witness set of an algebraic set X, it is straightforward to find *pseudo-witness sets* for its projections just by re-aligning the linear space L with various coordinate directions [24]. The re-alignment is done via continuation, tracking the witness point set as this proceeds. The number of continuation paths whose projections stay finite at the end of this process is the degree of the projected set, which may be smaller than the degree of the original set. The results are numerically equivalent to the symbolic elimination of variables.

While the main algorithms of numerical algebraic geometry compute solutions over the complex numbers, for applications, one is interested primarily in real solutions. For isolated solution points, one merely picks out the solutions with negligible imaginary parts. (In floating point complex numerical computation, the imaginary part will rarely be exactly zero even if the true solution it approximates is real.) For algebraic curves, the situation is more difficult. One can slice the curve with a real hyperplane and obtain real sample points on the curve, but even slicing many times,

[2] If the set has multiplicity μ, these points appear also with multiplicity μ.

one might miss interesting parts of the curve. There also can be ambiguity in how the points should connect to form the complete curve. A more secure, albeit more costly, treatment is to form equations for sweeping a real slicing plane parallel to itself and to solve for all the critical points where the plane touches the curve tangentially [21], or the curve has a cusp or singularity. These critical points include all the places where the real curve starts, stops, or crosses itself, and if they exist, even finds isolated real points on the complex curve. Between these critical points, the real arcs of the curve can be parametrized nonsingularly with respect to the sweeping coordinate, so they can be sampled numerically to any desired resolution.

3 Formulation of the (M, N) Alt-Burmester Problem

Each Alt-Burmester problem can be formulated such that the first precision pose is automatically attained, and eight freedoms remain to satisfy the other task prescriptions. As we shall see shortly, each additional precision pose consumes two freedoms because both path-point and orientation are specified, while each additional precision path-point consumes just one. Accordingly, for generic precision poses and precision points, the dimension D of the solution to the (M, N) problem is

$$D = 10 - 2M - N. \tag{1}$$

In particular, there are five distinct problems for which $D = 0$; specifically, there generically exists a finite number of solutions to problems $(5, 0)$, $(4, 2)$, $(3, 4)$, $(2, 6)$, and $(1, 8)$. Since the $(1, 8)$ problem has only one one pose and only relative orientation matters, this problem is equivalent to Alt's nine-path-point problem. Additionally, there are four synthesis problems for which there generally exists a curve of real solutions: problems $(4, 1)$, $(3, 3)$, $(2, 5)$, and $(1, 7)$, the last being equivalent to the eight-path-point problem.

We derive the polynomial system for these problems using *isotropic coordinates* [18]. Hence, we treat vectors as lying in the complex plane, such that a vector (v_x, v_y) in a standard Cartesian formulation becomes $(\mathbf{v}, \overline{\mathbf{v}}) = (v_x + i\, v_y, v_x - i\, v_y)$ in an isotropic formulation.[3] In the equations below, we follow the convention of [2], in which vectors in the fixed reference frame are capitalized, and vectors in the moving reference frame of the coupler link are lower case. Vectors encoded as complex numbers are in boldface, as are their complex conjugates that complete the isotropic coordinate pair.

A pair of planar RR dyads, each consisting of a proximal and distal link are shown in Fig. 2, with corresponding vector notation. For each of the two dyads, denoted by the subscripts 1 and 2, the to-be-determined locations of the fixed pivots are offset relative to an arbitrary fixed frame F by $\mathbf{G}_1$ and $\mathbf{G}_2$. The to-be-determined

[3] In interpreting solutions expressed in isotropic coordinates, one should note that v_x and v_y are real if and only if $\mathbf{v}$ and $\overline{\mathbf{v}}$ are complex conjugates.

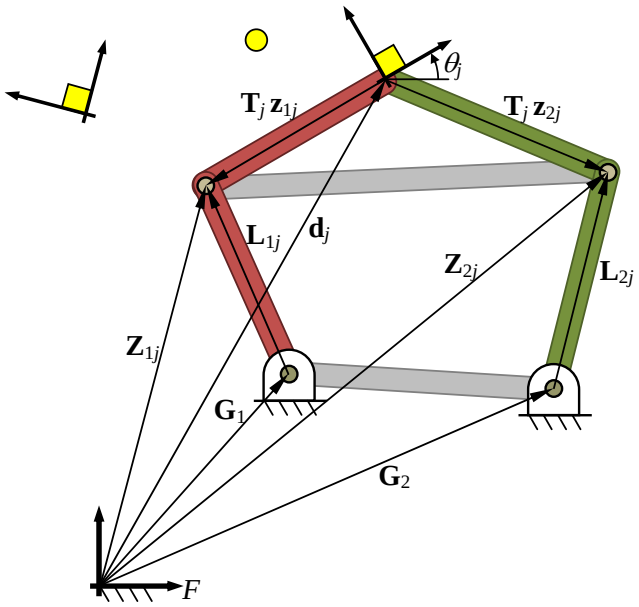

Figure 2: Vector diagram of a four-bar at the j^{th} pose. The yellow squares and circle indicate precision poses and a path-point, respectively.

lengths of the proximal links are L_1 and L_2. The position of the proximal links at the j^{th} pose are represented by $\mathbf{L}_{1j}$ and $\mathbf{L}_{2j}$. The location of the moving pivots (also known as the circle points) relative to a precision point, considered as vectors in the moving frame of the coupler link, are $\mathbf{z}_1$ and $\mathbf{z}_2$. The j^{th} pose is described relative to F by a frame consisting of a location vector $\mathbf{D}_j$ and an orientation angle θ_j. A precision path-point does not come with an angle. Dimensional synthesis of a four-bar linkage amounts to determining appropriate values of $\mathbf{G}_1$, $\mathbf{G}_2$, $\mathbf{z}_1$, and $\mathbf{z}_2$.

Let the precision data be numbered such that indices $j = 1, \ldots, M$ correspond to poses and $j = M+1, \ldots, M+N$ correspond to path-points. For all j, with respect to a fixed coordinate frame, the position of the coupler point is a vector $(\mathbf{D}_j, \overline{\mathbf{D}}_j)$ while the orientation of the coupler link is angle θ_j. All $(\mathbf{D}_j, \overline{\mathbf{D}}_j)$, $j = 1, \ldots, M+N$ are given, as are the angles of the poses, θ_j, $j = 1, \ldots, M$. The orientation of the coupler link at the path-points is not given and must be included in the variables of the problem. The orientations are expressed as a complex vector in polar form as $\Theta_j = \cos\theta_j + i\sin\theta_j = e^{i\theta_j}$. Since we are using isotropic coordinates, we also introduce a corresponding conjugate vector, $\overline{\Theta}_j$. If the j^{th} precision datum is a pose, then Θ_j and $\overline{\Theta}_j$ are given. For a path-point, these are unknowns, but they are not independent, as they must satisfy the unit-length identity:

$$\Theta_j\overline{\Theta}_j - 1 = 0, \qquad j = M+1, \ldots, M+N. \tag{2}$$

From the vector diagram of Fig. 2, one sees that the circle point $\mathbf{Z}_{1j}$ on dyad 1

can be written as

$$\mathbf{Z}_{1j} = \Theta_j \mathbf{z}_1 + \mathbf{D}_j, \tag{3}$$

and also

$$\mathbf{Z}_{1j} = \mathbf{G}_1 + \mathbf{L}_{1j}. \tag{4}$$

Combining these and writing the corresponding equation for the conjugate, we have, for $j = 1, \ldots, M+N$,

$$\mathbf{L}_{1j} = \Theta_j \mathbf{z}_1 + \mathbf{D}_j - \mathbf{G}_1, \tag{5}$$

$$\bar{\mathbf{L}}_{1j} = \overline{\Theta}_j \bar{\mathbf{z}}_1 + \overline{\mathbf{D}}_j - \overline{\mathbf{G}}_1. \tag{6}$$

The fundamental synthesis equation guarantees that the length of the proximal link remains constant at all times. That is, for $j = 2, \ldots, M+N$,

$$\mathbf{L}_{1j}\bar{\mathbf{L}}_{1j} - \mathbf{L}_{11}\bar{\mathbf{L}}_{11} = 0. \tag{7}$$

Similar equations can be formulated for the second RR dyad, which forms a second set of synthesis equations, these being, for $j = 1, \ldots, M+N$,

$$\mathbf{L}_{2j} = \Theta_j \mathbf{z}_2 + \mathbf{D}_j - \mathbf{G}_2, \tag{8}$$

$$\bar{\mathbf{L}}_{2j} = \overline{\Theta}_j \bar{\mathbf{z}}_2 + \overline{\mathbf{D}}_j - \overline{\mathbf{G}}_2, \tag{9}$$

along with, for $j = 2, \ldots, M+N$,

$$\mathbf{L}_{2j}\bar{\mathbf{L}}_{2j} - \mathbf{L}_{21}\bar{\mathbf{L}}_{21} = 0. \tag{10}$$

An accounting of the unknowns is as follows. In isotropic coordinates, the vector description of the linkage at the first precision datum has 8 variables, namely $\mathbf{G}_1$, $\mathbf{G}_2$, $\mathbf{z}_1$, $\mathbf{z}_2$ and their conjugates, $\overline{\mathbf{G}}_1$, $\overline{\mathbf{G}}_2$, $\bar{\mathbf{z}}_1$, $\bar{\mathbf{z}}_2$. Additionally, for each pose and path-point, we have unknowns $\mathbf{L}_{1j}, \mathbf{L}_{2j}$ and their conjugates $\bar{\mathbf{L}}_{1j}, \bar{\mathbf{L}}_{2j}$. Finally, for N path-points, the rotation coordinates $(\Theta_j, \overline{\Theta}_j)$ are unknown. This gives $8+4(M+N)+2N$ unknowns in total.

An accounting of the equations is as follows: Eq. (2), for $j = M+1, \ldots, M+N$; Eqs. (5),(6),(8),(9), for $j = 1, \ldots, M+N$; and Eqs. (7),(10), for $j = 2, \ldots, M+N$. For general precision data, the expected dimension of the solution set for the (M, N) Alt-Burmester problem is the total number of variables minus the total number of equations, which is $10 - 2M - N$ as in (1).

Some simplifications can be performed which leave the expected dimension of the solution set unchanged. For example, Eqs (5),(6),(8),(9) can be used to eliminate $\mathbf{L}_{1j}$, $\mathbf{L}_{2j}$, $\bar{\mathbf{L}}_{1j}$, $\bar{\mathbf{L}}_{2j}$ from Eqs. (7),(10). This reduces the number of unknowns and equations both by $4(M+N)$.

4 Complete solution of the (M, N) problem

We use numerical algebraic geometry to study the complete family of Alt-Burmester problems, reporting the degree of the solution set and the degree of its projections onto the center point and circle point coordinates. For the four cases that have in general a solution curve, we find not only the generic degrees of the curve and its center-point and circle-point projections but also the generic number of critical points of these curves. These indicate how many times the curve might reverse direction, which is a crucial step in plotting a curve. Section 5 considers a few particular examples of these curves and illustrate them with plots.

Although we solve the problems using a complete set of variables, namely

$$\{\mathbf{G}_1, \mathbf{G}_2, \mathbf{z}_1, \mathbf{z}_2, \overline{\mathbf{G}}_1, \overline{\mathbf{G}}_2, \overline{\mathbf{z}}_1, \overline{\mathbf{z}}_2, [(\Theta_j, \overline{\Theta}_j), j = M+1, \ldots, M+N]\},$$

we report on the degree of its projection onto the eight "natural" variables

$$\{\mathbf{G}_1, \mathbf{G}_2, \mathbf{z}_1, \mathbf{z}_2, \overline{\mathbf{G}}_1, \overline{\mathbf{G}}_2, \overline{\mathbf{z}}_1, \overline{\mathbf{z}}_2\}.$$

In the (M, N) combinations that give a zero-dimensional solution set, this degree is an upper bound on the number of real solutions that any problem in that class can have. The degree of the projections of the solution set onto just the center point coordinates of dyad 1, $(\mathbf{G}_1, \overline{\mathbf{G}}_1)$, and separately onto just the circle point coordinates of that dyad, $(\mathbf{z}_1, \overline{\mathbf{z}}_1)$, are often less than that of the original set.

4.1 Dimension and degree of the solution set

For each case (M, N), we used `Bertini` to solve a generic problem in which the precision data was randomly selected complex numbers. The results, with probability one, describe the general behavior of the solution sets, in particular, their dimension and degree. Table 1 gives these for the solution set in the eight natural variables, whereas Tables 2 and 3 give them for the center-point and circle-point projections, respectively. Singular solutions, which correspond to degenerate four-bars, are not included in these counts. Except for the $(4, 0)$ case, whenever the dimension of the solution set was at least 2, the closure of the projection onto the center point and circle point filled the entire space. These cases are indicated with an asterisk in Tables 2 and 3. In all the tables, the columns correspond to the number of poses, M, and the rows correspond to the number of path-points, N.

The degree of a zero-dimensional solution set is the number of solutions. For positive-dimensional solution sets, the degree is the number of intersection points of the component with a random slice, which is an invariant. The degree also gives some measure of how complex is the solution set. Degree 1 corresponds to linear components.

Table 1: Dimension and degree of Alt-Burmester solution sets, projected onto all eight natural variables.

		M									
		1		2		3		4		5	
N	0	8	1	6	4	4	16	2	16	0	16
	1	7	7	5	24	3	64	1	48		
	2	6	43	4	134	2	194	0	60		
	3	5	234	3	552	1	362				
	4	4	1108	2	1554	0	402				
	5	3	3832	1	2388						
	6	2	8716	0	2224						
	7	1	10858								
	8	0	8652								

Table 2: Dimension and degree of Alt-Burmester solution sets, projected onto the center point coordinates, $(\mathbf{G}_1, \overline{\mathbf{G}}_1)$.

		M									
		1		2		3		4		5	
N	0		$*$		$*$		$*$	1	3	0	4
	1		$*$		$*$		$*$	1	3		
	2		$*$		$*$		$*$	0	60		
	3		$*$		$*$	1	128				
	4		$*$		$*$	0	402				
	5		$*$	1	816						
	6		$*$	0	2224						
	7	1	3500								
	8	0	4326								

4.2 Problems having 0-dimensional solution sets

In Table 1, one sees that the number of solution points for the problems having zero-dimensional solution sets ranges from 16 for the (5,0) problem to 8652 for the (1,8) problem. These extremes are equivalent to Burmester's five-pose problem and Alt's nine path-point problem, respectively.

We have already noted that Burmester showed that the solution set of the five-pose problem consists of four dyads. Since the general formulation we use solves for both dyads simultaneously, these show up in Table 1 as $4 \cdot 4 = 16$ four-bars, but the projection onto either the center point or the circle point of dyad 1 gives the

Table 3: Dimension and degree of Alt-Burmester solution sets, projected onto the circle point coordinates, $(\mathbf{z}_1, \overline{\mathbf{z}}_1)$.

		M									
		1		2		3		4		5	
N	0		*		*		*	1	3	0	4
	1		*		*		*	1	3		
	2		*		*		*	0	60		
	3		*		*	1	142				
	4		*		*	0	402				
	5		*	1	1002						
	6		*	0	2224						
	7	1	5124								
	8	0	8652								

expected count of 4. Of the 16 solutions, the 4 that have dyad 1 equal to dyad 2 will not form true four-bars. The remaining 12 give just 6 different four-bars, since switching the numbering on the two dyads counts as a different solution to the polynomial system but makes no difference to the four-bar.

The other extreme, Alt's $(1, 8)$ problem, also shows a difference in degree amongst the three tables, but this time only the center-point projection is lower. As was observed in [14], the 8652 solutions of this problem appear with two symmetry actions: they appear in triplets according to Roberts cognates and each of these appears twice just by reversing the numbering of the two dyads. Thus, there are only 4326 distinct four-bars, appearing as 1442 Roberts cognate triplets. However, it is known that the center points of a Roberts cognate triplet form a triangle similar to the coupler triangle, see, for example, Fig. 78 in [8]. Since there are only three center points, under the six-way symmetry group, the projection onto $(\mathbf{G}_1, \overline{\mathbf{G}}_1)$ repeats twice, giving just 4326 distinct points. Meanwhile, in the same Fig. 78 in [8], one sees that there are six circle points, so the projection onto $(\mathbf{z}_1, \overline{\mathbf{z}}_1)$ does not repeat.

4.3 Problems having 1-dimensional solution sets

There are four Alt-Burmester problems that have a 1-dimensional family of mechanisms satisfying generic precision points. In these cases, a witness set for the solution curve consists of complex points, and as briefly mentioned in Sec. 2, it takes extra work to describe the set of real points that exist in the complex curve. The first step in computing a cell decomposition of the real curve is to find the critical points of the curve with respect to a sweeping hyperplane. The number of complex critical points with respect to a general sweep direction is a natural invariant of the curve, and we report on that here. To obtain the real cell decomposition for real precision

data, one can begin by computing the curve's real critical points using parameter continuation from the complex critical point set. For each problem, Table 4 lists the number of critical points with respect to a general projection for three different curves: the curve in the eight natural variables; the center-point curve $(\mathbf{G}_1, \overline{\mathbf{G}}_1)$; and the circle-point curve $(\mathbf{z}_1, \overline{\mathbf{z}}_1)$.

Table 4: Numbers of critical points for all one-dimensional Alt-Burmester problems with respect to polynomial system from Sec. 3.

(M, N)	Generic number of critical points					
	All 8 natural variables		$(\mathbf{G}_1, \overline{\mathbf{G}}_1)$		$(\mathbf{z}_1, \overline{\mathbf{z}}_1)$	
$(1, 7)$	55676	4168	38740	4168	44208	4168
$(2, 5)$	11228	988	8084	988	8456	988
$(3, 3)$	1440	144	972	144	1000	144
$(4, 1)$	152	16	92	16	92	16
	nonsingular	singular	nonsingular	singular	nonsingular	singular

4.4 Burmester's (4,0) problem

One other case in these tables gives a result that deserves explanation. Case (4,0) is Burmester's four-pose problem. As in any problem with only pose data and no path-points, the two dyads can be solved independently, and in fact their solution sets are identical. Due to this independence, when projected onto either the center point or the circle point coordinates, the two-dimensional solution set of case (4,0) becomes just one-dimensional. As shown in Tables 2 and 3, the center-point curve and the circle-point curve are each cubics, as was found by Burmester long ago.

Any problem of type $(M, 0)$ should be solved taking advantage of Burmester's technique of separating the two dyads. We report the results for these cases using the general formulation only for completeness.

5 Examples

The following present three examples of solving Alt-Burmester problems. All computations were done using `Bertini` to obtain solution points or witness sets and `Bertini_real` to extract real curves.

5.1 0-dimensional solution set – a $(4, 2)$ problem

The $(4, 2)$ problem has a zero dimensional solution set for generic parameter values. Table 5 contains randomly chosen values for the poses and points, which are used for the discussion here.

Table 5: Alt-Burmester task consisting of 4 poses and 2 path-points

j	d_{j_x}	d_{j_y}	θ_j (deg)
1	15.95	29.38	102.07
2	19.84	32.66	91.72
3	26.90	34.41	–
4	32.66	32.93	–
5	37.40	29.06	53.52
6	40.00	26.59	30.45

The problem has 60 complex solutions, of which 18 are real. The center points of the solutions must lie on the center-point curve of the associated $(4, 0)$ problem obtained by dropping the two path-points. In Fig. 3a, the locations of the center points for the (4,2) problem are shown in blue superimposed on the cyan center-point curve of the (4,0) problem, along with the four poses. Picking any one of the center points for dyad 1 automatically picks a corresponding center point for dyad 2 from the same set, thus the 18 center points correspond to just 9 distinct four-bar solutions. These 18 solutions are closely clustered in projection onto the center point. In Fig. 3b, we show how one of the solutions achieves the four poses and two path-points. The particular solution points used are at $\mathbf{G}_1$, $\mathbf{G}_2$ in Fig. 3a.

5.2 1-dimensional solution set – a $(4, 1)$ problem

The $(4, 1)$ Alt-Burmester problem generically has a 1-dimensional solution set of four-bar linkages. Table 6 gives specific parameter values we use in this example.

Table 6: Task specification with four poses and one point

j	d_{j_x}	d_{j_y}	θ_j (deg)
1	22.13	11.54	−24.15
2	20.98	22.88	6.93
3	10.45	23.44	–
4	5.23	27.17	54.14
5	−5.66	24.14	78.02

Computing a numerical irreducible decomposition using `Bertini` reveals that the algebraic variety in all of the variables for any (4,2) problem has two irreducible components of dimension one: one of degree 16 and the other of degree 72. As we will explain, the degree 16 piece is degenerate, so we ignore it. The degree 72 piece projects to a degree 48 curve in the eight natural variables, so this is the number

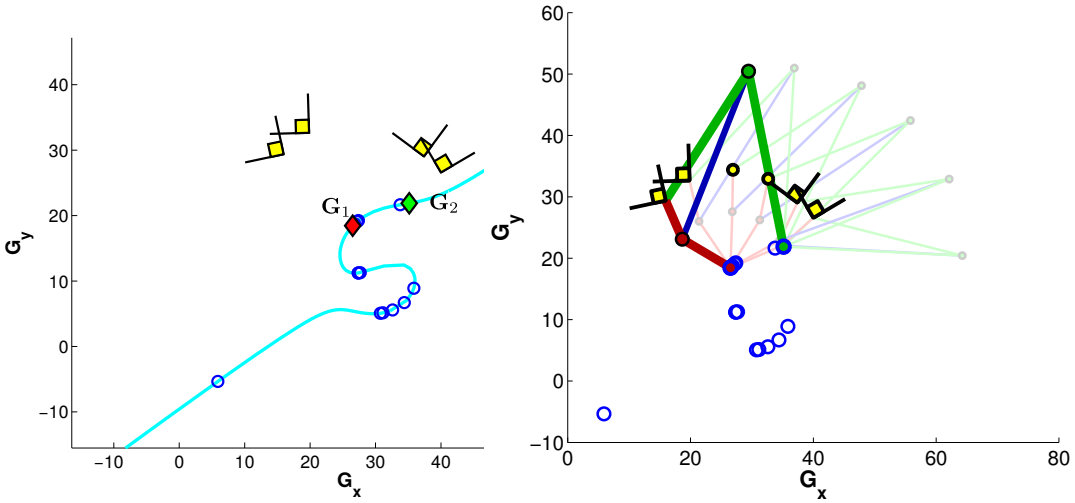

(a) The solution set for the $(4, 2)$ Alt-Burmester problem in Table 5.

(b) Demonstration mechanism corresponding to solution $\mathbf{G}_1$, $\mathbf{G}_2$.

Figure 3

reported in Table 1. Both components are self-conjugate, and hence potentially contain real curves.

As in the (4,2) case, the results for the (4,1) case can be better understood by considering the center-point curve of the associated (4,0) problem. This time, the (4,1) problem has a solution curve and it projects to exactly cover the (4,0) center-point curve. But the (4,1) problem and the associated (4,0) problem do not have the same solution set. The difference is that for the (4,0) problem, one can pick any two points on the center-point curve to form a four-bar. For the (4,1) problem, the choice for one center point must be matched by one of a finite set of center points for the other dyad such that the resulting four-bar will reach the extra path-point.

The degenerate degree 16 component occurs because one possibility for the second center point is to choose it exactly the same as the first one. This gives a four-bar mechanism that has degenerated to a planar RR mechanism.

The other solution component, the degree 72 curve, contains the nondegenerate solutions of the problem. Projecting this curve onto the eight natural variables yields a degree 48 curve.

So far, these comments apply to any general (4,1) problem. For the particular problem of Table 6, since it has real precision data, we may wish to find the real points in its solution curve. The first step in computing a cellular decomposition of the curve is to find its real critical points with respect to a sweep direction, including turning, cusp, or singular points. To do so, we could use a 'parameter continuation' from the critical point computation reported in Table 4, where it was found that (4,1) problems have in general 152 nonsingular and 16 singular critical points. However,

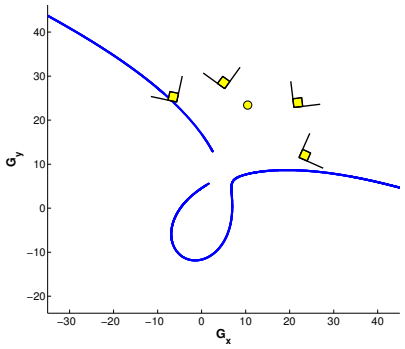

Figure 4: A projection of the solution curve for the $(4, 1)$ Alt-Burmester example problem. There is an interval where no mechanism may be constructed.

to numerically track the singular points would require 'desingularization', so instead we use the facility in `Bertini_real` to directly compute the critical points for this particular problem. The number of real points among these varies with the choice of a sweep direction, so while these are crucial to computing a real cell decomposition, their number is not of direct interest.

When the real arcs of the (4,1) curve have been computed in the full set of coordinates, the curve can be drawn in any projection. Fig. 4 shows the projection onto the center-point coordinates. Curiously, although the entire (4,1) solution curve projects to cover the entirety of the related (4,0) center-point curve, the real points of the (4,1) curve do *not* cover all the real points of the (4,0) center-point curve; as seen in the figure, there is a gap. This surprising fact has a straightforward explanation: in the gap, there are real points of the (4,0) curve that reach all four poses, but to reach the specified path-point, the coupler link must take a non-real rotation angle. The condition limiting the reach to the path-point is that one of the RR dyads has its proximal and distal links parallel. For dyad 1, this is written

$$\Theta_j \mathbf{z}_1 \overline{\mathbf{L}}_{1j} - \overline{\Theta}_j \overline{\mathbf{z}}_1 \mathbf{L}_{1j} = 0. \tag{11}$$

where j is the index of the path-point. (In this example, $j = 3$.) Accordingly, one can find these workspace boundary mechanisms by adding Eq. (11), for the appropriate j to the synthesis constraints of Eqs. (2), (7) and (10). Among the solutions to this system, there are several such that $\mathbf{G}_1$ corresponds with one of the boundary points of the gap on the center-point curve. Furthermore, since $(\mathbf{z}_2, \overline{\mathbf{z}}_2)$ do not enter the boundary condition Eq. (11), it is not necessary to include Eqs. (10); instead, it suffices to solve Eqs. (2), (7) and (11), a system of six equations in six unknowns, $(\mathbf{G}_1, \mathbf{z}_1, \Theta_5, \overline{\mathbf{G}}_1, \overline{\mathbf{z}}_1, \overline{\Theta}_5)$. In this pared-down system, each boundary point appears just once. A similar system formed for dyad 2 gives the same result, as must be the case since the numbering of the dyads is arbitrary.

5.3 1-dimensional solution set − a $(3,3)$ problem

As a final example, we consider synthesizing a four-bar mechanism to guide a rigid body through the 3 task poses and 3 path-points given in Table 7. Using `Bertini_real`, we computed a cellular decomposition of the solution curve. The projection of this curve onto the center-point plane is shown in Fig. 5. According to Table 2, this projection is a curve of degree 128, while Table 4 gives the generic number of critical points in the different projections we have been discussing. Similar to the (4,1) problem, picking one center point $\mathbf{G}_1$ from this curve determines a finite number of locations for the other center point, $\mathbf{G}_2$. These points must also lie on this same center-point curve.

Table 7: Task combination with 3-poses and 3-points

j	d_{j_x}	d_{j_y}	θ_j
1	-72.67	39.91	72.51
2	-20.22	10.00	15.21
3	57.82	53.08	-63.51
4	5.06	70.00	–
5	-13.32	46.20	–
6	15.22	50.28	–

Figure 5 shows the center-point curve at three different scales. Zoomed far out, Fig. 5a accentuates the asymptotes to infinity of the curve. These appear as 12 asymptotes, defining 24 rays. A center-point at infinity means that the associated circle point moves on a circle of infinite radius, which makes these points equivalent to a slider joint. Each asymptote corresponds to one point at infinity, so we see that the solution set for the particular (3,3) problem under consideration includes 12 PRRR-type four-bars. One could, of course, set up a new problem to solve for these directly: an Alt-Burmester (3,3) problem for slider-cranks.

Zooming in twice produces Figs. 5b and 5c that show more details of the curve. Especially in Fig. 5c, one may notice that there are three points in the plane where the center-point curve has multiple self-crossings. Further investigation shows that these points seem to be related to the three precision poses and are not dependent on the three path-points. In particular, the self-crossings coincide with the poles of the three poses. This is illustrated in Fig. 5d, which shows just the three precision poses and their poles. At present, we have no further explanation for this phenomenon, but we conjecture that the center-point curve of any (3,3) Alt-Burmester problem has self-crossings at the vertices of the related pole triangle.

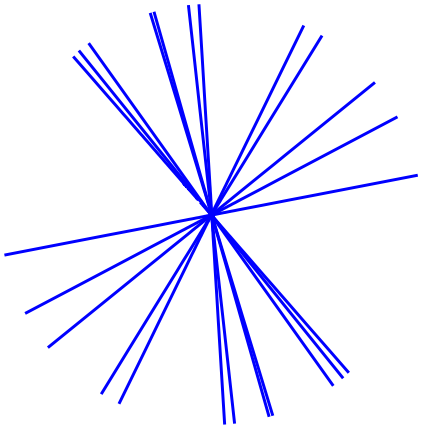

(a) Far out view, showing 12 asymptotes to infinity.

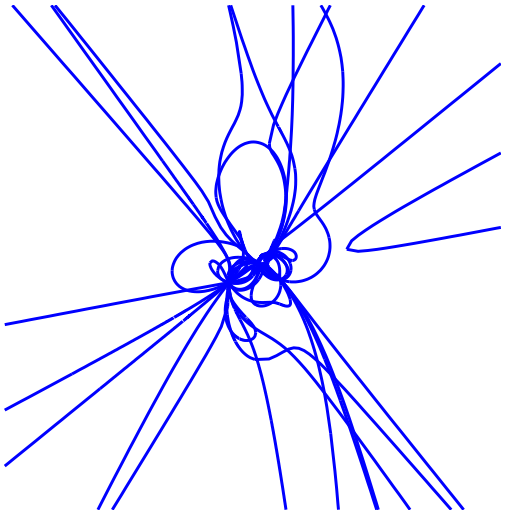

(b) Zoom showing how the asymptotes transition into the curve.

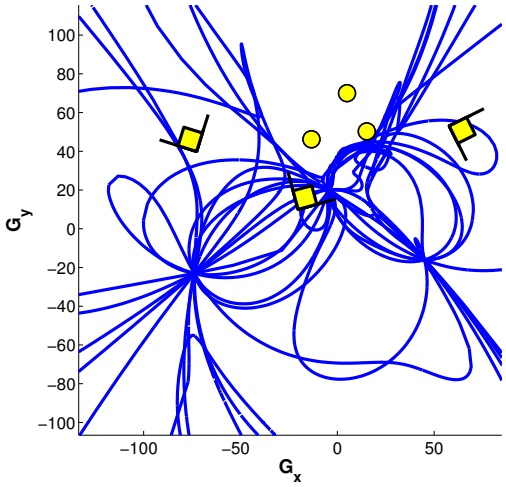

(c) The apparent crossings of the curve in this close-up correspond to the pole triangle in (d).

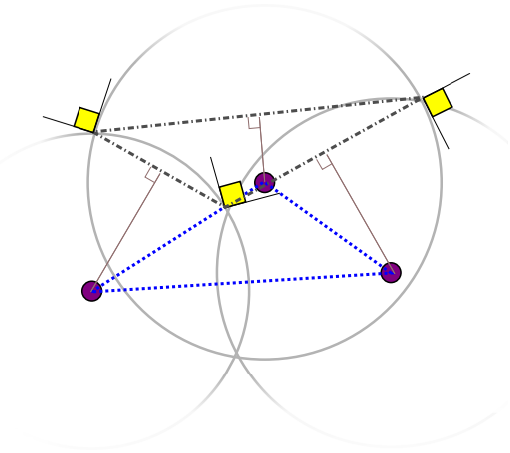

(d) The pole triangle.

Figure 5: Plots of the $(3, 3)$ Alt-Burmester problem from Table 7, projected onto the center point of dyad 1.

6 Conclusions

We have studied all the (M, N) Alt-Burmester problems using numerical algebraic geometry as implemented in the `Bertini` software package. We give the dimension and degree of the solution set for every general case from the trivial (1,0) problem that has an 8-dimensional solution, up to the five cases that have 0-dimensional solutions. The 0-dimensional cases, which include Burmester's five-pose problem, case (5,0), and Alt's nine path-point problem, case (1,8), have degrees ranging from 16 to 8652. Those extremes had been settled before, but the mixed cases in between, namely (4,2), (3,4), and (2,6), are newly treated. The four cases with solution curves have been investigated in more depth to the extent of determining the general number of critical points of each, a step that is useful in plotting the real arcs of these curves. The (1,7) curve is the most difficult one in the set, having, in the natural 8 coordinates, a degree of 10,858 and approximately five times that number of critical points. For the more tractable cases of the (4,1) and (3,3) problems, we give illustrations of the center-point curves for a specific example of each and point out interesting features of these.

7 Acknowledgments

DAB and JDH were supported in part by DARPA Young Faculty Award, NSF ACI-1460032, and Sloan Research Fellowship. CWW was supported in part by NSF ACI-1440607.

References

[1] Erdman, A., Sandor, G., and Kota, S., 2001, *Mechanism Design: Analysis and Synthesis*, Vol. 1, 4/e, Prentice-Hall, Englewood Cliffs, NJ.

[2] McCarthy, J.M., and Soh, G.S., 2011, *Geometric Design of Linkages*, 2/e, Springer-Verlag, New York.

[3] Sandor, G., Erdman, A., 1984, *Advanced Mechanism Design: Analysis and Synthesis*, Vol. 2, Prentice-Hall, Englewood Cliffs, NJ.

[4] Balli, S.S. and Chand, S., 2002, "Defects in Link Mechanisms and Solution Rectification", Mech. Mach. Theory, **37**(9), pp. 851-876.

[5] Tong, Y., Myszka, D.H., and Murray, A.P., 2013, "Four-Bar Linkage Synthesis for a Combination of Motion and Path-Point Generation", Proceedings of the ASME International Design Engineering Technical Conferences, Paper No. DETC2013-12969.

[6] Alt, H., 1923, "Über die Erzeugung gegebener ebener Kurven mit Hilfe des Gelenkvierecks", ZAMM, **3**(1), pp. 13–19.

[7] Burmester, L., 1886, *Lehrbuch der Kinematic*, Verlag Von Arthur Felix, Leipzig, Germany.

[8] Bottema, O., and Roth, B., 1990, *Theoretical Kinematics*, Dover Publications, Mineola, NY.

[9] Freudenstein, F. and Sandor, G., 1959, "Synthesis of Path Generating Mechanisms by Means of a Programmed Digital Computer", ASME J. Eng. Ind., **81**(1), pp. 159–168.

[10] Suh, C. and Radcliffe, C., 1966, "Synthesis of Path Generating Mechanisms with Use of the Displacement Matrix", Proceedings of the ASME International Design Technical Conferences, 66-MECH-19, pp. 9-19.

[11] Morgan, A. and Wampler, C., 1990, "Solving a Planar Fourbar Design Problem Using Continuation", ASME J. Mech. Des., **112**(4), pp. 544-550.

[12] Roth, B., and Freudenstein, F., 1963, "Synthesis of Path-Generating Mechanisms by Numerical Means", ASME J. Eng. Ind., **85**(3), pp. 298–306.

[13] Tsai, L.-W., and Lu, J.-J., 1989, "Coupler-Point-Synthesis Using Homotopy Methods", *Advances in Design Automation—1989: Mechanical Systems Analysis, Design and Simulation*, B. Ravani, ed., ASME DE-Vol. 19-3, pp. 417–424.

[14] Wampler, C.W., 1992, "Complete Solution of the Nine-Point Path Synthesis Problem for Fourbar Linkages", ASME J. Mech. Des., **114**(1), pp. 153-161.

[15] Tsai, L.W. and Morgan, A.P., 1985, "Solving the Kinematics of the Most General Six- and Five-Degree-of-Freedom Manipulators by Continuation Methods", ASME J. Mech., Trans., Automation, **107**(2), pp. 189–200.

[16] Raghavan, M., 1993, "The Stewart Platform of General Geometry has 40 Configurations", ASME J. Mech. Des., **115**(2), pp. 277–282.

[17] Sommese, A.J., Verschelde, J., and Wampler, C.W., 2004, "Advances in Polynomial Continuation for Solving Problems in Kinematics", ASME J. Mech. Des., **126**(2), pp. 262–268.

[18] Wampler, C.W., and Sommese, A.J., 2011, "Numerical Algebraic Geometry and Algebraic Kinematics", Acta Numerica, **20**, pp. 469–567.

[19] Sommese, A.J., and Wampler, C.W., 2005, *Numerical Solution of Systems of Polynomials Arising In Engineering And Science*, World Scientific Press, Singapore.

[20] Bates, D.J., Hauenstein, J.D., Sommese, A.J., and Wampler, C.W., 2013, *Numerically Solving Polynomial Systems with Bertini*, Software, Environments, and Tools 25, SIAM, Philadelphia, PA. Software available at bertini.nd.edu.

[21] Lu, Y., Bates, D.J., Sommese, A.J., and Wampler, C.W., 2007, "Finding All Real Points of a Complex Curve", Contemp. Math. **448**(8), pp. 183–205.

[22] Brake, D.A., Bates, D.J., Hao, W., Hauenstein, J.D., Sommese, A.J., and Wampler, C.W., 2014, "Bertini_real: Software for One- and Two-Dimensional Real Algebraic Sets", *Mathematical Software - ICMS 2014*, Springer, pp. 175–182. Software available at bertinireal.com.

[23] Morgan, A.P., and Sommese, A.J., 1989, "Coefficient-Parameter Polynomial Continuation", Appl. Math. Comput., **29**(2), pp. 123–160. Errata, 1992, *Appl. Math. Comput.*, **51**, pp. 207.

[24] Hauenstein, J.D. and Sommese, A.J., 2010, "Witness Sets of Projections", Appl. Math. Comput., **217**(7), pp. 3349–3354.